ORIGINAL PAPER

Experimental Study on Energy Evolution and Failure Characteristics of Rock–Coal–Rock Combination with Different Height Ratios

Bao Pan · Weijian Yu ⓘ · Wenbing Shen

Abstract Compared with the surrounding rock of single rock roadway, the uneven deformation of surrounding rock of thin coal seam roadway is more prominent. This uneven deformation characteristic of thin coal seam surrounding rock between the different surrounding rocks has greatly hindered the mining of thin seam coal mines. Based on the uniaxial loading tests and uniaxial cyclic loading tests of the coal–rock combination, the deformation characteristics and loading failure of coal–rock combination with different height ratios of coal to rock is studied. The results show that the uniaxial compression strength of coal–rock combinations increases with coal height. By comparing and analyzing the energy evolution of the composite with different height ratio, the energy dissipation of the coal–rock combination decreases suddenly between RCR-0.5 and RCR-1 specimens. The coal body is constrained by the sandstone at both ends of the composite specimen, which improved the strength of the coal body. The effect of this constraint decreases with the distance from the coal–rock interface. The failure mode of the composite specimens is dominated by the coal body, which is from splitting failure to shear failure finally becomes middle coal extrusion.

1 Introduction

In the thin coal seams, the surrounding rock of mining roadway often presents in the form of coal and rock. The problem of large non-uniform deformation in roadway is caused by the difference of mechanical properties between coal body and rock body. Therefore, various laboratory tests and analyses of coal–rock composite samples for rock mechanics have studied by scholars at home and abroad. According to different geological conditions of the sites, the mechanical properties and failure forms of different combinations such as coal–rock, rock–coal and rock–coal–rock have been studied to provide theoretical basis for thin coal seam mine (Kulhawy 1975; Yu et al. 2019a, b, 2020). As the result of compression tests on different combinations of coal and rock shown, the uniaxial compression strength, elastic modulus and impact energy index of the combination is greatly

B. Pan · W. Yu (✉) · W. Shen
School of Resource and Environment and Safety Engineering, Hunan University of Science and Technology, Xiangtan 411201, China
e-mail: ywjlah@163.com

W. Yu
Hunan Provincial Key Laboratory of Safe Mining Techniques of Coal Mines, Hunan University of Science and Technology, Xiangtan 411201, China

influenced by the position of the coal body (Lan et al. 2018). Under the same coal rock height ratio, the conclusion that the order of combination strength and acoustic emission energy from large to small is coal–rock, rock–coal, rock–coal–rock was summarized by the means of FLAC2D (Zhou et al. 2019). The loading energy distribution of composite specimens with different height ratio and different diameter shows that most accumulated energy is concentrated in the softer rock layer. With the increase of the height ratio of coal–rock combination, the peak energy of coal–rock combination and the energy ratio of coal component gradually increases (Chen et al. 2020).

The compression strength, deformation characteristics, crack evolution and post peak strength of coal rock combination under different confining pressures was completely analyzed (Zuo et al. 2016; Chen et al. 2018; Song et al. 2018). By studying the failure characteristics of coal rock assemblages with different dip angles, the anchoring function and mechanism of coal–rock-anchor combination are summarized (Yu et al. 2019a, b, 2020). The numerical model of coal–rock combination with different height ratio is established by FPC particle flow software. And the result of the numerical simulation shows that the failure mode of the coal–rock combination is mainly reflected in the coal part. With the decrease of the coal part, the failure mode changes from a single shear crack to a V-shaped crack, and the end surface effect of the coal part get increasingly significant. The deformation and failure process of the combination failure is a typical progressive failure process (Nie and Zhou 2018). Furthermore, the mechanical model is established to fit and predict the deformation of surrounding rock (Liu et al. 2018). Based on the assumption that the rock mass of the compressed rock–coal–rock combination is regarded as a spring structure, a criterion for judging the impact failure of the rock–coal–rock combination is proposed (Tang and Xu 1991; Mu et al. 2013). The impact tests of rock–coal–rock combination and coal–rock–coal combination at different strain rates were carried out by split Hopkinson pressure bar (SHPB). And the results show that the stress–strain curve increases rapidly in a straight line at the initial loading stage of the composite. When the stress rises to about 75% of the peak stress, the slope of the curve decreases gradually until the failure with the increase of the stress (Miao et al. 2019).

The mechanical properties and deformation and failure laws of coal rock combinations are studied from different perspectives by the above researches. In order to further analyze the mechanical properties of different rock layers and reveal the non-uniform deformation characteristics of rock coal combination, indoor test analysis is carried out for rock–coal–rock combination.

2 Materials and Methods

2.1 Preparation of Specimens

The rock materials of sandstone and coal for this experiment were collected from Linli Country in Hunan province, China. The stones with good integrity and no obvious crack are polished to a cylinder with a diameter of 50 mm and a height of different, which the parallelism of the two ends of each cylinder must be < 0.02 mm. The two same-high sandstone cylinders and one coal cylinders were bonded in the sequence of sandstone-coal-sandstone to φ50 mm × 100 mm standard test specimens with high intensity marble adhesive. The ratios of the coal height to the total sandstone height of these specimens are 0.25: 1, 0.5: 1, 1: 1 and 2: 1. These specimens are divided into 4 groups according to coal–rock height ratio: RCR-0.25, RCR-0.5, RCR-1 and RCR-2. The specimens are marked serial number in each group, for example: RCR-0.25-1, RCR-0.25-2, RCR-0.25-3 RCR-0.25-4, RCR-0.25-5 and RCR-0.25-6. Each group of specimens was separately used for uniaxial compression test and uniaxial cyclic compression test. And the most typical test piece data in each group is selected for subsequent analysis.

2.2 Uniaxial Compression

The process of uniaxial compression test is made of two stages, uniaxial one-time loading and uniaxial cyclic loading. In this study, the RMT-150C rock mechanics test system is used to apply axial pressure to the specimen. The uniaxial one-time loading test were carried out to obtain the mechanical parameters of the combinations for subsequent experiment. The method of loading is load controlling, which is loading to the failure of the specimen with rate 0.05 KN/s. During the loading process, strain gauges are pasted on the sides surface of the sandstones and the coal body. The strain gauges with Digital Signal Processor (DSP)

are used to monitor the real-time deformation of each part of the combination (Fig. 1).

According to the coal–rock height ratios from low to high, the peak strength σ_1 of each group of rock–coal–rock composites obtained by the uniaxial one-time loading test are: 72.0 KN, 67.4 KN, 60.4 KN and 53.0 KN, respectively. And the uniaxial compression strength σ_1 of the different height ratio specimens are shown in Fig. 2. From the figure, the uniaxial compression strength of the combination decreases with the increase of coal rock height (Fig. 3).

The uniaxial compression peak strength obtained by the uniaxial one-time loading was used to cyclically loading. In the first loading cycle, the axial force on these specimens was unloaded to 5 KN after respectively loading to 70% of the corresponding uniaxial peak strength. And the loading peak value of the next cycle is increased by 5% σ_1eσ_1 until the loading peak value to 95% of the peak strength. Eventually, these specimens were loaded to failure after the final cycle. The compression mode of cyclically loading is controlled by loading value which is in the wave of "Slope shape + Triangle". Therefore, the initial
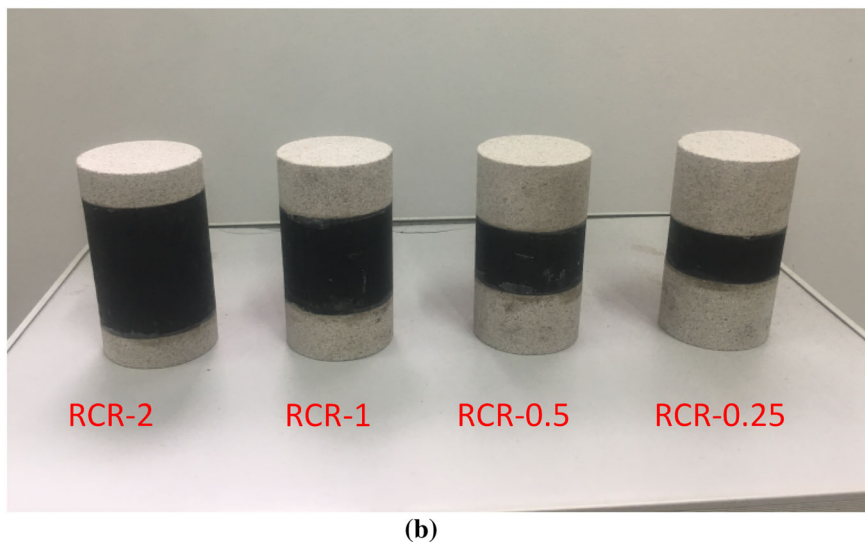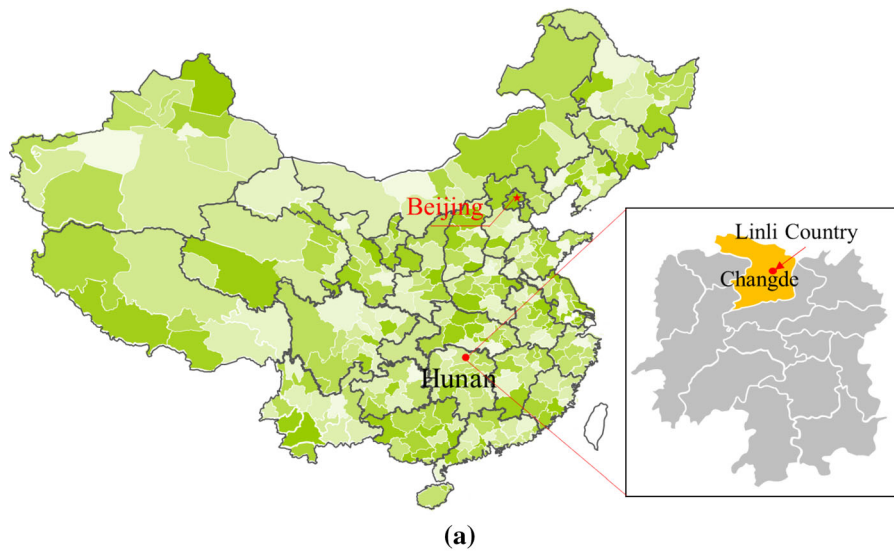

(a)

RCR-2   RCR-1   RCR-0.5   RCR-0.25

(b)

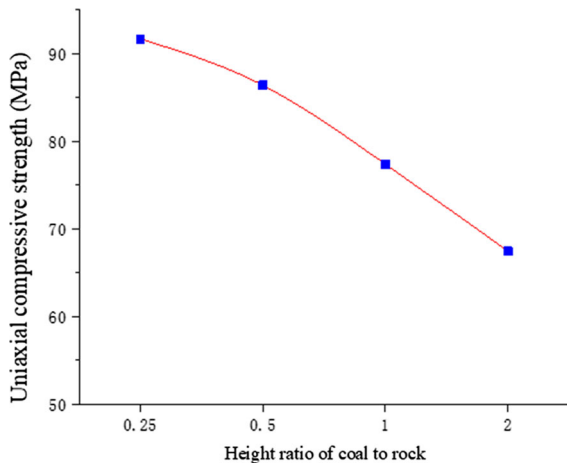**Fig. 1** Preparation of specimens **a** sampling area map **b** standard test piece

Fig. 2 Uniaxial compression strength of combination with different height ratios of coal to rock
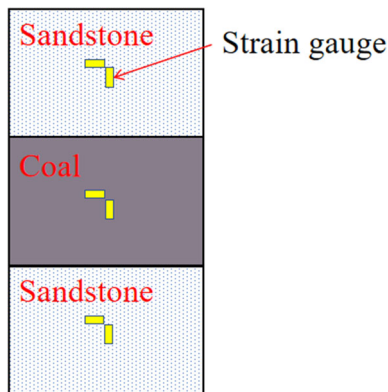

Fig. 3 The location of strain gauge

loading rate in a single cycle is 0.05 KN/s before loading to the average value. Then, the wave shape of load is changed to a triangular waveform with a frequency of 0.001/s. In the triangular loading process, the load of the test piece decreases to 5 KN, after increases to the peak value of the cycle, and enters the next cycle. After the last cycle, the test piece is loaded to failure with loading rate 0.05 KN/s.

3 Mechanical Properties of Rock–Coal–Rock Combination

3.1 Deformation Analysis

Due to the difference in the mechanical properties of sandstone and coal bodies, when the combination

system is under load, the axial strain ε_1 and lateral strain ε_2 of the sandstone parts at both ends and the middle coal body are significantly different. In order to study deformation process of the rock–coal–rock combination under loading, pairs of mutual vertical strain gauges are attached to the center of the side surface of each rock bodies. These strain gauges are used to monitor the deformation of the center of the three parts (upper sandstone, lower sandstone and coal body).

The stress–strain curves of the middle parts of the sandstone and coal in combination are shown in Fig. 4 (due to the deformation of the upper and lower sandstones is definitely similar, the stress–strain curves of the lower sandstone are omitted). The initial increase rate of strain increases rapidly. As the load increases, increase rate of the axial strain decreases and finally get linearly. This phase is particularly obvious on sandstone. Otherwise, the sandstone axial strains and lateral strains are significantly smaller than the axial and lateral strains of the coal body. And the compression-shear bonding strength of this adhesive is reach to 10.3 MPa, especially, the failure patterns of specimens show the conclusion that even if the whole coal rock assemblage is destroyed, there is no relative sliding of coal rock interface. During the loading process, the middle parts of the three parts of combination are expanding respectively. Meanwhile, the coal and sandstones are bonded by high intensity adhesive which restrict the two sides of the structure surface to slide relatively. Thus, when the rock–coal–rock combination is loaded, the lateral deformation of different parts affects each other through the coal–rock structural plane, which finally shows the non-uniform deformation of the combination specimen under compression. The general lateral deformation state of rock–coal–rock combination is small-large-small.

During a period of time before the failure, namely, the end of the stress–strain curve, lateral strain curve of the sandstone upwarp obviously, while the axial strain curve still presents linear changing. This shows that the deformation of sandstone is significantly affected by the coal before the failure of the composite specimen, which does not deform according its Poisson's ratio.

It can be seen from previous studies that the failure process of the coal rock combination is as follow: The initial macro cracks are generated in the coal body. Then, these cracks extend to the sandstone body, and
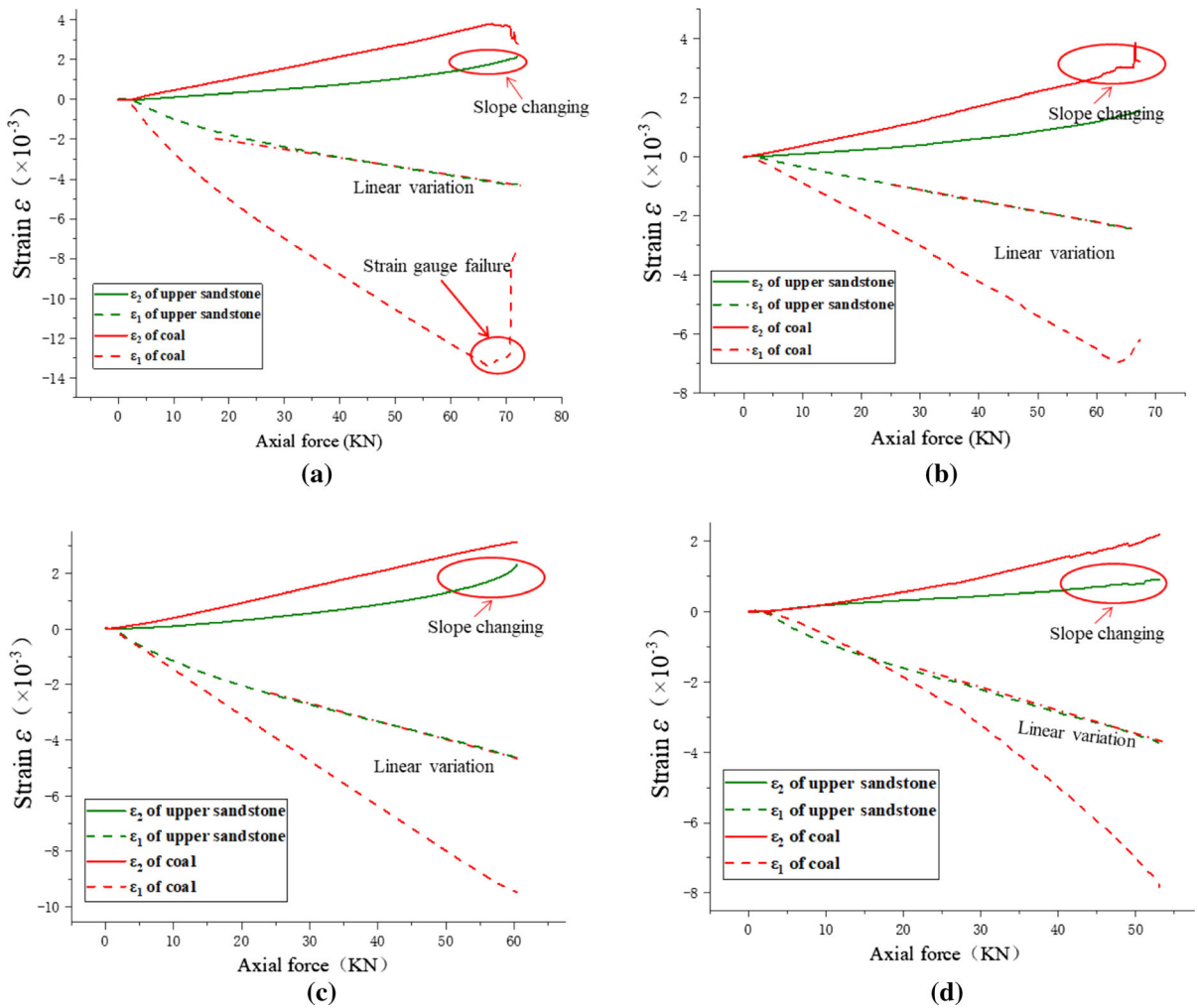
Fig. 4 Stress–strain curve of each part of coal rock combinations a RCR-0.25, b RCR-0.5, c RCR-1 and d RCR-2

finally cause the overall failure of the specimen. Combined with the mentioned deformation characteristics of the rock–coal–rock combination, the conclusion is drawn: during the compression, the coal body lateral expansion is constricted by the coal–rock interface.

3.2 Mechanical Model of Rock–Coal–Rock Combination

Each part of the combination specimens deforms separately, which is caused by the difference in mechanical properties between coal and rock. In the loaded combination system, lateral strain of the sandstone at both ends of the combination is smaller

than lateral strain of the coal. Meanwhile, the sandstone-coal interface limits the relative sliding between the rocks on both sides. Therefore, the trend of lateral expansion of coal body near the coal–rock interface is restricted by sandstone when they are compressed. The circumferential inward shear stress is generated by this constraint, which gradually decreases as it is far away from the coal rock contact surface. The stress model of the compression specimen is shown in Fig. 5. In the rock–coal–rock combination with low height ratio, the distribution of the internal shear stress of the coal body starts to decrease from both ends, then overlaps in middle part, and the overall change is relatively smooth. However, as the height of coal increase, the internal shear stress of the coal body

gradually decreases from both ends to zero. The constraint of the middle part disappears, where the relative weak zone is generated in that position (Fig. 6).

The heterogeneous shear stress distribution of the coal sections determines the great relationship between the strength of rock–coal–rock combination and coal height. When the coal body is subjected to the maximum axial principal stress, the shear stress exerted by the coal–rock interface take the function as confining pressure on the coal body, which improve the strength of the coal body. Therefore, compared with the coal specimen, the uniaxial compressive strength of the rock–coal–rock combination specimen is improved by the circumferentially inward shear stress. Moreover, this enhancement of uniaxial compressive strength is related to the coal height: when the height of coal body is small, the uniaxial compressive strength of coal with little internal change is enhanced obviously; As the height of coal body increase, the relative weak zone is generated in middle part of coal where the uniaxial compressive strength is low.

4 Energy Evolution

4.1 Internal Energy Analysis

In the uniaxial cyclic loading experiment, the energy of the combination system is divided into four parts:

input energy, accumulated energy, dissipated energy and released energy. The energy input of combination system is the work done by the axial press on the test specimen. A part of the energy is accumulated as elastic energy in coal body and sandstone body. And the rest of input energy is dissipated to internal damage, plastic deformation (Yang et al. 2019). The formula is drowned as follow:

$$U = U_e + U_p \tag{1}$$

where U is input energy, U_e and U_p is dissipated energy and released energy, respectively.

The strength of coal is much lower than sandstone uniaxial compressive strength. Hence, the sandstone is still in the stage of linear elastic deformation before the ultimate failure of coal. Based on the assumption that high strength sandstone is regarded as spring structure, there is only reversible elastic energy accumulation in sandstone, and all energy for plastic deformation and damage are dissipated in coal. According to the stress–strain curve of the cyclic loading test, during the loading and unloading process of a certain cycle, the unloading curve is not the same as the original path and is lower than the loading curve. The analysis method for this cycle is: the area under the loading curve is the work done U of the external load on the combination, the area under the unloading curve is the elastic energy U_e released by the combination and the dissipated energy in coal U_p is
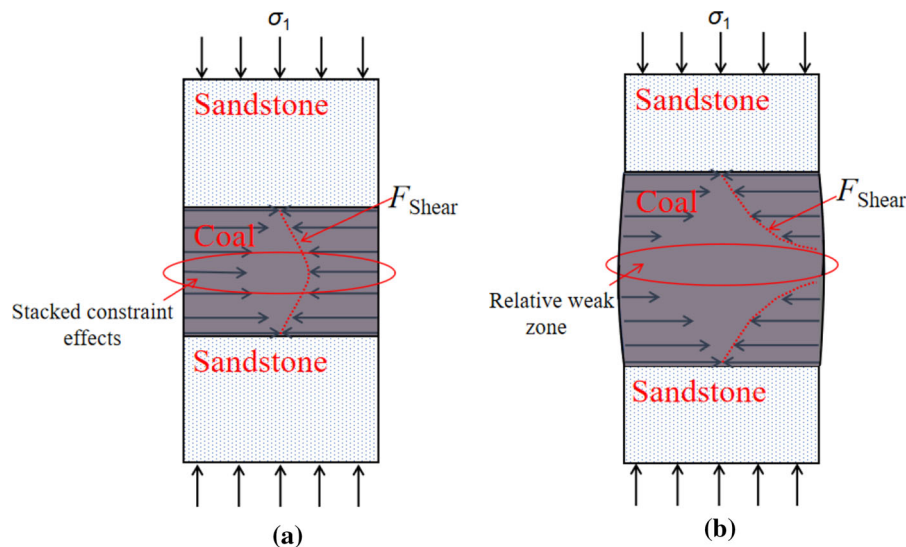

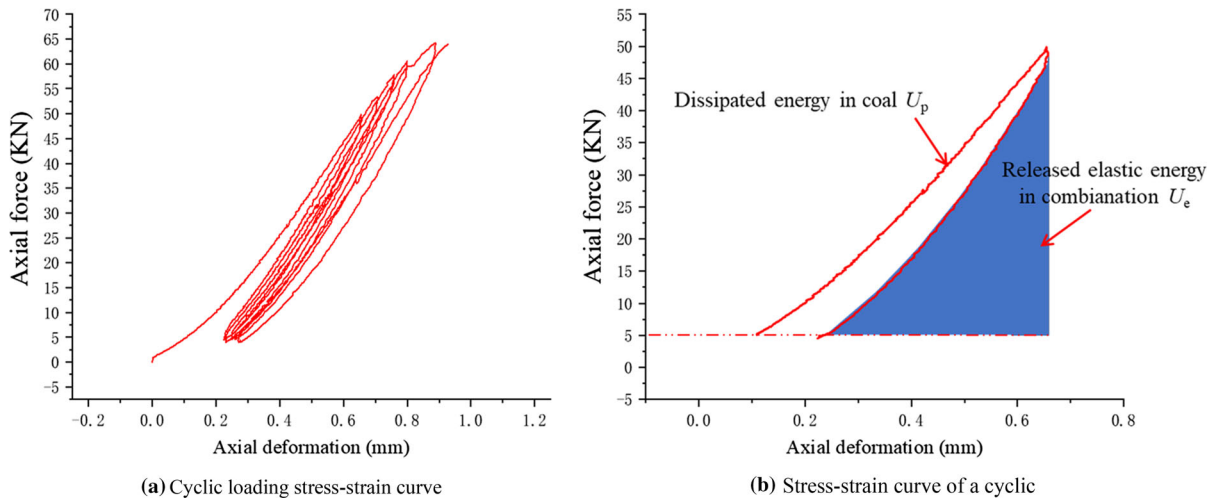Fig. 5 Shear stress distribution of composite specimen a RCR-0.5 b RCR-1

(a) Cyclic loading stress-strain curve

(b) Stress-strain curve of a cyclic

Fig. 6 Energy analysis model of coal rock combination. a Cyclic loading stress–strain curve b stress–strain curve of a cyclic

Table 1 Uniaxial loading strength and loading parameters of composite (KN)				

Specimen group	RCR-0.25	RCR-0.5	RCR-1	RCR-2
Compression peak strength	72.0	67.4	60.4	53.0
70%				
Peak value	50.4	47.2	42.3	37.1
Average value	27.7	26.1	23.7	21.1
Amplitude	45.4	42.2	37.3	32.1
75%				
Peak value	54.0	50.6	45.3	39.8
Average value	29.5	27.8	25.2	22.4
Amplitude	49.0	45.5	40.3	34.8
80%				
Peak value	57.6	53.9	48.3	42.7
Average value	31.3	29.5	26.7	23.2
Amplitude	52.6	48.9	43.3	37.4
85%				
Peak value	61.2	57.3	51.4	45.1
Average value	33.1	31.1	28.2	25.0
Amplitude	56.2	52.3	46.4	40.1
90%				
Peak value	64.8	60.6	54.4	47.7
Average value	34.9	32.8	29.7	26.4
Amplitude	59.8	55.4	49.4	42.3
95%				
Peak value	68.4	64.0	57.4	50.4
Average value	36.7	34.5	31.2	27.7
Amplitude	63.4	59.0	52.4	45.4

Table 2 Energy of different height ratio combinations in the stage of 70–95% of uniaxial compressive peak strength (J)

| Specimen group	Loading progress					
	70%	75%	80%	85%	90%	95%
RCR-0.25						
U	11.0280	11.5210	13.4461	14.8028	19.0418	
U_e	7.3160	8.9936	10.7797	11.9353	13.9624	
U_p	3.7120	2.5274	2.6664	2.8675	5.0794	
RCR-0.5						
U	10.8483	10.8947	13.6647	14.6962		
U_e	7.5600	8.7490	10.5899	11.9074		
U_p	3.2883	2.1457	3.0748	2.7888		
RCR-1						
U	9.2709	9.6753	10.9909	12.2654	14.1512	16.0969
U_e	6.9192	7.9463	9.3024	10.4111	12.0502	13.8762
U_p	2.3517	1.7290	1.6885	1.8543	2.1010	2.2207
RCR-2						
U	9.4063	9.7339	11.2596	12.8484	14.4022	16.5193
U_e	7.0717	8.1853	9.4443	10.9523	12.2394	14.1679
U_p	2.3346	1.5486	1.8153	1.8961	2.6280	2.3514
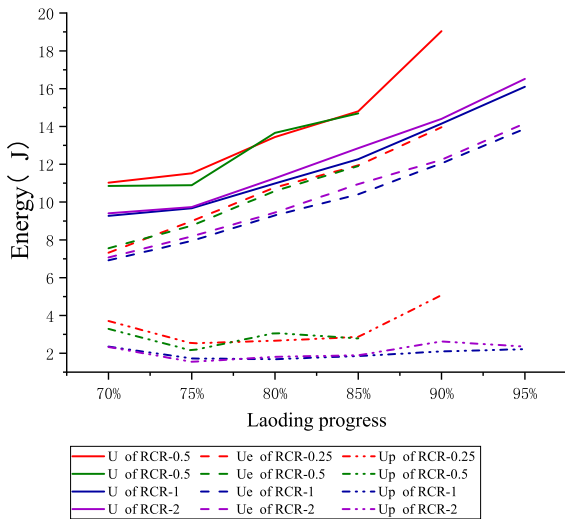
Fig. 7 Energy evolution process of combination

the area where is encircled by the loading curve and unloading curve (Table 1).

4.2 Energy of Combinations with Different Height Ratio

Graphic integration method is used to compute the input energy, dissipated energy and released energy in the cycles of 70–90%. The results are shown in Table 2. (The blank grid is the result of failure of the uniaxial compression strength at the place where some specimens fail to reach the one-time uniaxial loading, and no data is obtained.)

The energy evolution process of each group specimens in the above Table 2 are compared, and the results are shown in Fig. 7. All the input energy density and released elastic energy density increase with the increase of peak load. The energy factors such as input energy U, dissipated energy U_e and released energy U_p between the low height ratio groups RCR-0.25 and RCR-0.5 and high height ratio groups RCR-1 RCR-2 are different obviously: energy of the specimen with the gradual increase of the coal body height caused a bluff type change in the process of the coal–rock height ratio from 0.5:1 to 1:1. Base on assumption that the coal body is homogeneous, the maximum value of dissipated energy in per unit volume of coal body is certain. Consequently, in the process of increasing the coal–rock height ratio from 0.5:1 to 1:1, the coal body height which began to release dissipated energy inside the composite decrease.

Due to the restriction from both ends, the deformation of the coal body in the loading system tends to be small at both ends and large in the middle. As a result, the internal energy release process of the compressed specimen is asynchronous at all coal
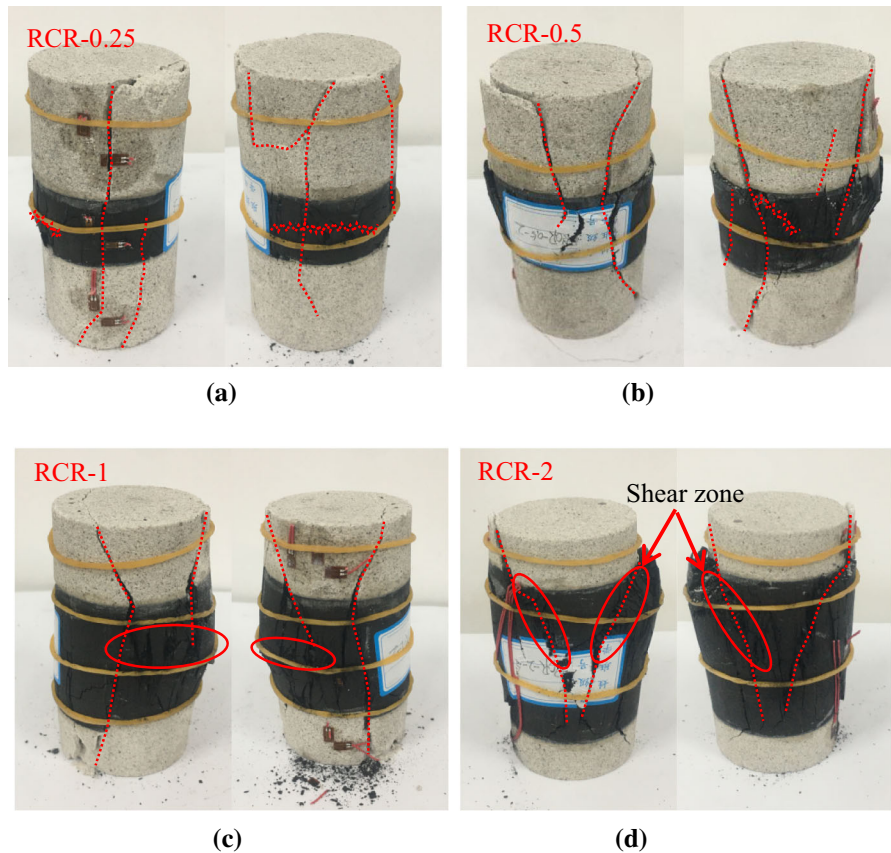
Fig. 8 Classical failure modes of specimens with different height ratio. **a** RCR-0.25. **b** RCR-0.5. **c** RCR-1. **d** RCR-2

sections. According to the stress state in coal body, with the lateral deformation of the coal body, the internal cracks are generated and developed, and the energy stored in the coal body is dissipated. Hence, when the plastic deformation occurs in the coal body, the middle part of the high coal body starts to dissipated energy, moreover, the parts at both ends have not yet started to release energy. However, the general deformation of the coal body with small height is consistent, and the volume of coal body with fracture development and energy release at the same time is more.

5 Failure Characteristics of Combination

According to the failure mode of each height ratio combination, as shown in Fig. 8, it can be seen that the integrity of specimens with various coal height after failure is distinctive. Among them, RCR-0.25

specimen is the best integral, and the main cracks are distributed both in sandstone and coal, which angles are vertical, and the dense and even fissures are distributed on the coal side surface. The inclined main cracks are distributed on sandstones and coal of RCR-0.5 combination which has superior integrity. Fissures on the coal side surface of this combination are concentrated on the area between the mains cracks; For RCR-1, specimens present a loose integral after failure. Only two main cracks are distributed on the sandstone part with large dip angle, and the coal body on side of the main crack expands outwards; From the fragmented RCR-2 combination after failure, the coal body is extruded out with the main crack as the boundary, and the both of sandstones is virtually complete. Furthermore, shear zones are spread on the main cracks which is structural dislocations caused by the displacement of local coal body in elastic stage (Jiao et al. 2012)

The failure mode of the combination is changing with the increase of the coal–rock height ratio, which from splitting failure to shear failure finally becomes middle coal extrusion. With the increase of specimen load before the coal body enters into the plastic stage, the internal fissures are generated and developing. The stress distribution of the specimen with low coal–rock height ratio the fracture development degree of the all coal sections is uniform. For high coal–rock height ratio combination, the stress is concentrated in the middle part of the coal body. Before the failure, the relatively weak area of the middle part is caused by great stress gradient in the coal sections. The main cracks expand to both ends from the middle part of the coal body, furthermore, the part of coal slips and be extrude.

6 Conclusions

1. The unaxial compressive strength of rock–coal–rock combination is determined by the weak rock, coal. Compared with the simple coal samples, the constraint applied on coal improve the coal strength by changing the stress state in the coal body.

2. The decreasing circumferential shear stress is distributed in the coal body according the height ratio: the maximum shear stress decreases with the increase of the distance from the coal structure surface. Otherwise, in the coal body with low height, the shear stress overlaps in the middle part of the coal body; with the increase of the height of the coal body, the attenuation of the shear stress in the middle of the coal body decreases radically and the shear stress vacuum is generated.

3. The energy releasing in the coal body is asynchronous and related to the height of the coal body. In the high coal rock height ratio specimen, when the dissipated energy of the middle part reaches the maximum value, the energy of the coal body at ends is dissipated inadequately. However, the energy evolution process of the low coal rock height ratio specimen in consecutive sections is relatively consistent. Before the specimen failure, the energy is dissipated sufficiently.

References

Chen Y, Zuo JP, Song HQ et al (2018) Deformation and crack evolution of coal–rock combined body under cyclic loading-unloading effects. J Min Saf Eng 35(3):826–833

Chen GB, Qin ZC, Zhang GH et al (2020) Law of energy distribution before failure of loaded coal–rock combined body. J Rock Soil Mech 41(6):1–13

Jiao XF, Zhang WJ, Kang TH (2012) Meso simulation of formation and development of rock shear zone and its failure mechanism. J Coal Eng 2:104–107

Kulhawy FH (1975) Stress deformation properties of rock and rock discontinuities. J Eng Geol 9(4):327–350

Lan YW, Zhang GH, Liu HL et al (2018) Mechanical characteristics underlying coal and rock combinations under different combination conditions. J Heilongjiang Univ Sci Technol 28(2):136–141

Liu XS, Tan YL, Ning JG et al (2018) Mechanical properties and damage constitutive model of coal in coal–rock combined body. Int J Rock Mech Min Sci 110:140–150

Miao LG, Niu YY, Shi BM (2019) Impact dynamic tests for rock–coal–rock combination under different strain rates. J Vib Shock 38(17):137–143

Mu ZL, Wang H, Peng P et al (2013) Experimental research on failure characteristics and bursting liability of rock–coal–rock sample. J Min Saf Eng 30(6):841–847

Nie X, Zhou AC (2018) Numerical analysis on mechanical characteristics of coal–rock combination of different height ratios. J Coal Technol 37(3):102–104

Song HQ, Zuo JP, Chen Y et al (2018) Post-peak stress-strain relationship model and brittle characteristics of coal–rock combined body. J Min Saf Eng 35(5):1063–1070

Tang CN, Xu XH (1991) The whole process of rock fracture and the whole sequence of seismogenesis. J Acta Seismol Sin 13(4):517–522

Yang L, Gao FQ, Wang XQ et al (2019) Study on energy evolution law and failure mechanism of coal–rock combined specimen. J China Coal Soc. https://doi.org/10.13225/j.cnki.jccs.2019.0011

Yu WJ, Pan B, Zhang F et al (2019a) Deformation characteristics and determination of optimum supporting time of alteration rock mass in deep mine. J Civ Eng 23(11):4921–4932

Yu WJ, Wu GS, Liu Z et al (2019b) Experimental study on uneven failure of loose coal and rock composite specimen. J Coal Sci Technol 47(1):85–90

Yu WJ, Wu GS, Liu Z et al (2020) Uniaxial compression test of coal–rock–bolt anchorage body and mechanical mechanisms of bolts. Chin J Rock Mech Eng 39(1):57–68

Zhou CY, Liu CX, Ma DP et al (2019) Analysis of strength and acoustic emission characteristics of coal and rock mass in different combinations. J Saf Coal Mines 50(2):232–236

Zuo JP, Chen Y, Zhang JW et al (2016) Failure behavior and
    strength characteristics of coal–rock combined body under
    different con- fining pressures. J China Coal Soc
    41(11):2706–2713